Environmental Science & Technology Letters

pubs.acs.org/journal/estlcu

Letter

Enhanced Organic Nitrate Formation from Peroxy Radicals in the Condensed Phase

Victoria P. Barber,* Lexy N. LeMar, Yaowei Li, Jonathan W. Zheng, Frank N. Keutsch, and Jesse H. Kroll*

Cite This: *Environ. Sci. Technol. Lett.* 2024, 11, 975−980

Read Online

ACCESS | Metrics & More | Article Recommendations | Supporting Information

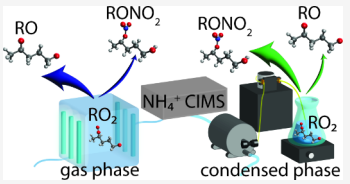

ABSTRACT: Organic alkoxy (RO) and peroxy (RO_2) radicals are key intermediates in multiphase atmospheric oxidation chemistry, though most of the study of their chemistry has focused on the gas phase. To better understand how radical chemistry may vary across different phases, we examine the chemistry of a model system, the 1-pentoxy radical, in three phases: the aqueous phase, the condensed organic phase, and the gas phase. In each phase, we generate the 1-pentoxy radical from the photolysis of *n*-pentyl nitrite, run the chemistry under conditions in which RO_2 radicals react with NO, and detect the products in real time using an ammonium chemical ionization mass spectrometer (NH_4^+ CIMS). The condensed-phase chemistry shows an increase in formation of organic nitrate ($RONO_2$) from the downstream RO_2+NO reaction, which is attributed to potential collisional and solvent-cage stabilization of the RO_2−NO complex. We further observe an enhancement in the yield of carbonyl relative to hydroxy carbonyl products in the condensed phase, indicating changes to RO radical kinetics. The different branching ratios in the condensed phase impact the product volatility distribution as well as HO_x-NO_x chemistry, and may have implications for nitrate formation, aqueous aerosol formation, and radical cycling within atmospheric particles and droplets.

KEYWORDS: *Alkoxy radicals, peroxy radicals, organic nitrate, organic aerosol, aqueous oxidation*

1. INTRODUCTION

The oxidation of organic species in the atmospheric condensed phase (aerosol particles and droplets) is a key chemical process with important implications for atmospheric composition. Multiphase oxidation alters the chemical composition and properties (hygroscopicity, optical properties, etc.) of particles, affects gas phase composition,[1] and can lead to the formation of secondary organic aerosol via reactions in cloud and aerosol water (aqueous organic aerosol (aqSOA)).[2−4] Such chemistry is thought to proceed via the same general mechanism as oxidation in the gas phase, in which the organic compound is attacked by an oxidant (e.g., the hydroxyl radical OH), leading to a sequence of reactions involving alkoxy (RO) and peroxy (RO_2) radicals, and ultimately forming closed-shell organic products.[5−8] However, radical chemistry in the condensed phase is substantially more complicated than in the gas phase due to the presence of the solvent, which can affect radical reactivity via effects such as collisional stabilization, direct involvement of solvent molecules, and changes to reaction thermodynamics and kinetics due to solvent−solute interactions.[9−11] These effects may lead to product distributions that are fundamentally different from those in the gas phase, and so may impact the composition of both the gas and particle phases.

Much of our understanding of condensed-phase organic radical chemistry is based on off-line studies of liquid-phase oxidation reactions, such as pulsed radiolysis measurements of the reaction of OH radicals with organic species in the aqueous phase[12−14] and on a limited number of online studies of liquid-phase oxidation.[15] A difficulty in interpreting results from such studies is the substantial chemical complexity associated with organic oxidation processes, particularly for large molecules: a single reaction step can form different organic radicals, high oxidant levels can lead to multiple generations of oxidation, and products can have multiple functional groups, posing analytical challenges.

Here we take an alternative approach for studying the condensed-phase chemistry of organic radicals, involving radical generation via direct photolysis. In particular, we explore the multiphase chemistry of a single organic radical, 1-pentoxy (C_5H_9O), generated from photolysis of a *n*-pentyl nitrite (PN) precursor:

$$CH_3(CH_2)_4ONO + h\nu \rightarrow CH_3(CH_2)_4O + NO \quad (R1)$$

Direct radical generation allows for the formation of a single radical isomer, which in comparison to traditional oxidant-initiated oxidation affords substantially simpler chemistry, and largely avoids unwanted secondary oxidation reactions.[16,17] We employ this approach in three different systems: the gas phase,

Received: June 20, 2024
Revised: August 6, 2024
Accepted: August 7, 2024
Published: August 13, 2024

the bulk organic condensed phase, and the bulk aqueous phase. Online detection of product species allows for the direct comparison of the chemistry of the 1-pentoxy radical (and its downstream intermediates, including RO_2 radicals) among these three phases.

2. METHODS AND MATERIALS

Different reactor setups are used to probe radical chemistry in different phases (see Figure S5). Condensed-phase experiments are conducted in a 10 mL borosilicate volumetric flask equipped with a magnetic stir bar. Hexafluorobenzene (C_6F_6, Sigma-Aldrich, NMR grade, > 99.5%), a nonpolar, aprotic molecule, is used as the solvent for the organic phase experiments. For aqueous experiments, 0.05 M, pH 7 phosphate buffer is used as the solvent to minimize the effects of RONO hydrolysis (see SI).[18] 0.125 μL of acetonitrile (Sigma-Aldrich, 99.8%) is added to each solution as a flow tracer (5.0 ppmv). 6.25 μL of PN (Sigma-Aldrich, > 95%) is then added to each solution (250 ppmv). The solution is continually mixed using a stir bar, ensuring that organics are homogeneously distributed in the bulk solution prior to and during photolysis; this also avoids depletion of O_2 within the solution. The solution is then photolyzed using a strip of UVA LEDs (λ = 365 nm, Waveform Lighting). Consistent with the product distributions (discussed below), the high concentration of RONO used in the experiments results in conditions in which the reactivity of RO_2 radicals is dominated by RO_2 + NO chemistry, with negligible contribution from other RO_2 reactions. The solution is introduced into an atomizer (Brechtel Manufacturing) using a peristaltic pump (ESI MP2) at a flow rate of 12 μL/min. The solution is converted to a fine spray which rapidly vaporizes as it is diluted with ~20 LPM of clean, dry air; analysis with a scanning mobility particle sizer (SMPS, TSI) shows no evidence of aerosol particles, indicating full vaporization. The diluted, vaporized effluent is sampled into the NH_4^+ CIMS for detection (see SI, including Figure S5). Several control experiments (see SI) indicate that tubing losses may contribute to a slight change in shape of the time traces, but this leads to negligible changes in product distributions. While the experiments are designed to probe bulk-phase chemistry, and observations are consistent with such chemistry, surface or bulk droplet-phase chemistry in the atomizer cannot be completely ruled out. Future experiments relying on liquid-phase analytical techniques could clarify the results further.

Gas-phase experiments are conducted in the MIT environmental chamber.[19] During experiments, a constant 5 LPM flow of zero air from a clean air generator (Aadco 737 Series) is introduced into the chamber to replenish the flow drawn by the instruments. To mimic the high NO concentrations accessed in the condensed-phase experiments, ~ 200 ppb of NO, monitored by a chemiluminescence NO−NO_2−NO_x analyzer (Thermo Scientific, Model 42i), are added. As in the condensed-phase experiments, observed products suggest that RO_2 reacts only with NO under these conditions; when no NO is added, the dominant products observed are consistent with RO_2 + HO_2 reactions (see SI). Acetonitrile is injected into the chamber as a dilution tracer. 45 ppb of the PN radical precursor are then injected into the chamber. The concentrations are allowed to stabilize for approximately 10 min, and then the UV-A lamps (centered at 340 nm) are switched on to initiate photolysis.

Reaction products generated in both setups are measured in real time using a time-of-flight NH_4^+ CIMS,[20] which is sensitive to a wide range of oxygenated VOCs. Given the uncertainty associated with calibration of the NH_4^+ CIMS, in this work we report CIMS measurements in terms of mass spectrometric signal (duty-cycle-corrected counts per second), normalized to the acetonitrile signal to correct for variations in flow. Because the CIMS sensitivity may vary from compound to compound, these values may not accurately reflect relative concentrations of the different species. We thus restrict our discussion to differences in concentrations between phases. The three experiments are performed using the same instrument under similar operating conditions; calibration factors for a given compound are the same and so signal intensities are directly comparable between experiments.

3. RESULTS AND DISCUSSION

Stacked plots depicting the time evolution of photochemical product ions observed in the three experiments (gas phase, organic condensed phase, and aqueous phase) are presented in Figure 1. Molecular formulas are detected as the analyte-NH_4^+

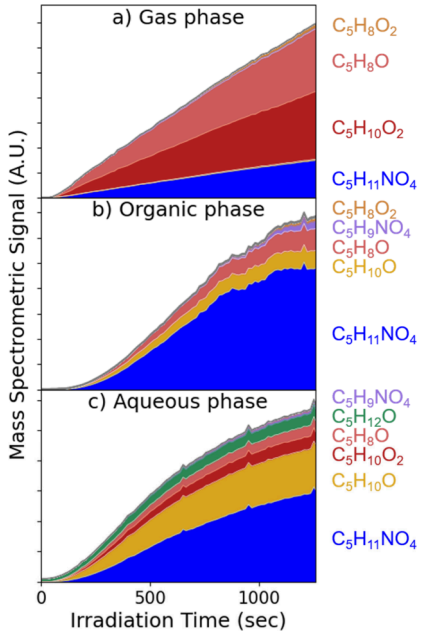

Figure 1. : Time-resolved mass spectrometric signals for *n*-pentyl nitrite photolysis products, in three phases: (a) the gas phase, (b) the condensed organic phase, and (3) the aqueous phase. All measurements use the NH_4^+ CIMS, and formulas listed are those of the analytes (products are detected as the complexes with NH_4^+). Signals are smoothed over 15-s intervals and normalized to the dilution tracer, acetonitrile; t = 0 refers to the time at which UV lights are switched on.

adduct unless otherwise noted, but are presented as the molecular formula of the analyte (omitting the NH_4^+). In all cases, products are consistent with the expected chemistry of the 1-pentoxy radical under RO_2 + NO conditions,[21,22] shown in Figure 2. No evidence of second-generation oxidation chemistry (e.g., due to OH formed from HO_2 + NO) is observed. The proposed mechanism accounts for all observed major products, though the presence of alternative pathways or minor products cannot be fully ruled out. The 1-pentoxy radical, formed from RONO photolysis, forms either a

https://doi.org/10.1021/acs.estlett.4c00473
Environ. Sci. Technol. Lett. 2024, 11, 975−980

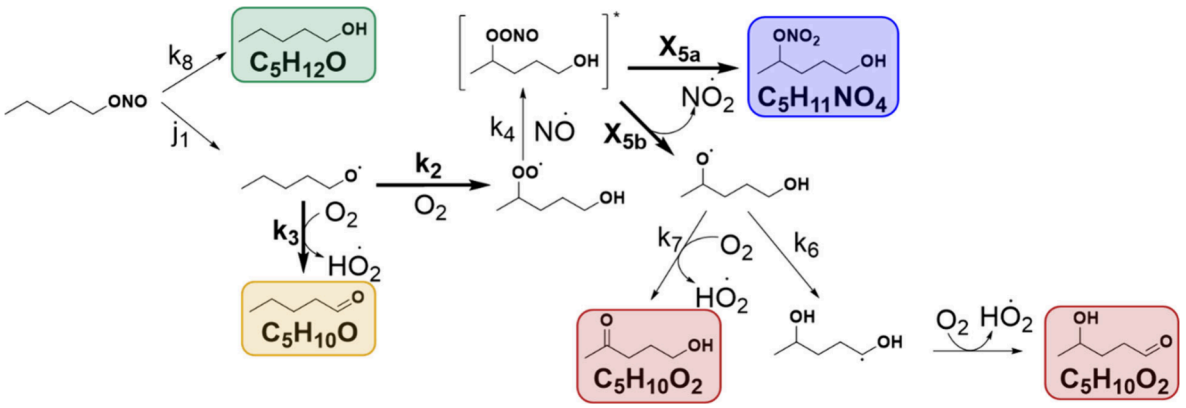

Figure 2. : Simplified reaction mechanism for the photolysis of *n*-pentyl nitrite. Detected closed-shell products are highlighted, with colors corresponding to the products shown in Figure 1.

Table 1. : Model Fitted Parameters for the Gas, Organic, and Aqueous Phase Photolysis of *n*-Pentyl Nitrite

Phase	Photolysis rate constant j_1 (s^{-1})	Hydrolysis rate constant k_8 (s^{-1})	Alkoxy radical branching ratio $k_3[O_2]/(k_3[O_2] + k_2)$	Nitrate branching ratio from RO_2 + NO X_{5a}
Gas	$(2.9 \pm 0.1) \times 10^{-4}$	N/A	$(6.6 \pm 0.4) \times 10^{-3}$	0.22 ± 0.001
Organic	$(4.3 \pm 0.6) \times 10^{-3}$	N/A	0.099 ± 0.008	0.86 ± 0.04
Aqueous	$(7.0 \pm 0.2) \times 10^{-5}$	$(1.6 \pm 0.7) \times 10^{-3}$	0.31 ± 0.007	0.79 ± 0.03

carbonyl ($C_5H_{10}O$) through reaction with O_2 or a hydroxyperoxy (RO_2) radical via isomerization. Under the conditions of these experiments, the RO_2 reacts with NO; this is thought to form a peroxynitrite intermediate, which either rearranges to form the hydroxy nitrate ($C_5H_{11}NO_4$) or dissociates to yield another RO radical, ultimately producing a hydroxycarbonyl ($C_5H_{10}O_2$). As both of these products are the result of the reaction between RO_2 and NO, the branching ratio between the two pathways is independent of NO concentration. Also observed in the gas-phase experiment is a species with formula C_5H_8O, consistent with the dehydration of the hydroxycarbonyl (see SI). One additional product, $C_5H_{12}O$, is observed in the aqueous phase only, and is likely the alcohol formed from the hydrolysis of the RONO precursor (see SI).[18]

Substantial differences in product distributions are observed between the experiments in different phases, with the most pronounced differences being between the gas phase and the two condensed phases. This implies differences in rates and branching ratios among phases, which we quantified by fitting time-dependent product signals to a kinetic model (see SI). Key rate constants and branching ratios are given in Table 1. As discussed further in SI, the alkoxy radical branching ratio and the nitrate yield given in Table 1 are derived from uncalibrated CIMS measurements, and hence may contain as much as a factor of 2−3 absolute error for individual values based on differing sensitivities for different products. However, calibration factors are likely to be the same in different phases, so uncertainties cancel out for the ratios reported in Table 2.

The most obvious difference in product distribution in the different phases is the organic nitrate ($C_5H_{11}NO_4$): this is a minor product in the gas-phase system (Figure 1a), as expected,[23] but is one of the most abundant products in the two condensed-phase systems (Figure 1b-c). This indicates a substantial difference in RO_2 + NO branching (R5) in different phases: as shown in Table 1, values of X_{5a} are a factor of 4 and 3.5 larger in the organic condensed phase and aqueous phase, respectively, than in the gas phase. To our knowledge, this enhanced nitrate formation has not previously been examined

Table 2. Literature Values for X_{5a} in the Gas and Aqueous Phases, and Enhancement Factor (Ratio of X_{5a} Values) between the Two Phases

Peroxy Radical	X_{5a}(g), 1 atm, 298 K	X_{5a}(aq), 298 K	X_{5a}(aq)/X_{5a}(g)
Methyl Peroxy	0.017 ± 0.0014[25]	0.23 ± 0.4[24] 0.86 ± 0.02[28]	14, 51
Ethyl Peroxy	0.033 ± 0.004[29]	0.67 ± 0.03[24]	20
Propyl Peroxy	0.038 ± 0.002[30,a] 0.036 ± 0.005[31,b]	0.71 ± 0.04[24,b]	19
Tert-Butanol Peroxy	0.044[23]	0.86 ± 0.02[28]	20
5-hydroxy-pentan-2-yl peroxy	0.13[23]	0.24[23]	1.8[23] 3.5[c]

[a]All values are taken from measurements, apart from italicized items which are calculated from the structure−activity relationship presented by Jenkin et al.[23] Reported value for isopropyl peroxy radical only. [b]Reported value for a combination of *n*-propyl and isopropyl peroxy radicals. [c]This work.

in the context of the atmospheric condensed phase (aerosol particles and droplets). However, earlier work examining RO_2 chemistry in other aqueous systems (e.g., seawater) has found similar enhancements in the $RONO_2$ yields from the RO_2 + NO reaction in the aqueous phase for a number of small RO_2 radicals.[24,25] Literature values for gas- and aqueous-phase $RONO_2$ branching ratios, as well as the enhancement factor in the aqueous phase (X_{5a}(aq)/X_{5a}(g)) are summarized in Table 2. Interestingly, the enhancement factor observed in this study is substantially lower than those observed for small, unsubstituted RO_2. One possible origin of this difference is the molecular structure of the RO_2 radical itself; future studies exploring the influence of RO_2 structure on the aqueous phase enhancement factor would provide further insight into this effect. By contrast, two previous studies on heterogeneous oxidation of liquid organic particles in the presence of gas-phase NO[26,27] observed no alkyl nitrate formation; this inconsistency may arise differences in experimental conditions

https://doi.org/10.1021/acs.estlett.4c00473
Environ. Sci. Technol. Lett. 2024, 11, 975−980

(e.g., oxidation from the gas phase rather that from within the condensed phase) and/or analytical approaches used.

The difference between gas- and condensed-phase $RONO_2$ branching ratios likely arises from differences in the dynamics of the ROONO intermediate, which can either rearrange to form $RONO_2$ or dissociate to RO + NO_2 (Figure 2).[32] The enhancement in $RONO_2$ yield in the condensed phase is consistent with the well-established increase in $RONO_2$ yields with pressure, which is likely due to collisional stabilization of the ROONO intermediate.[31−33] From the number concentration of water molecules, we can estimate an enhancement of X_{5a} in the aqueous phase using known pressure-dependences. We predict an enhancement of 1.8, qualitatively consistent with (but lower than) the enhancement of 3.5 observed in this experiment.

Another possible contributing factor is the solvent cage effect, which keeps the reactive fragment species (RO and NO_2) in close proximity, thereby increasing the potential for collisions and consequently the probability of recombination.[34] Previous work on a similar molecule, peroxynitrous acid (HOONO), has suggested that such an effect could play a role in preventing the decomposition to OH + NO_2 (analogous to the decomposition of ROONO to RO + NO_2).[35] Additional experimental and computational work is needed to better understand the roles of both collisional stabilization and the solvent cage effects on the phase-dependent $RONO_2$ yields.

The other major difference between the gas- and condensed-phase product distributions is the enhanced yield of the carbonyl species ($C_5H_{10}O$) in the condensed phase. This suggests a difference in the chemistry of the RO radical. In particular, the relative rate of reaction with O_2 and isomerization (i.e., $k_3[O_2]/k_2$) is enhanced by a factor of ∼16 for the condensed organic phase compared to the gas phase, an enhancement that increases to ∼69 for the aqueous phase (Table 1). The difference is not a result of differences in O_2 concentrations: from Henry's Law constants,[36] the O_2 concentrations in H_2O and C_6F_6 are a factor of 31 and a factor of 2 lower than in the gas phase, respectively, which should result in a decreased condensed-phase yield, contrary to observation.

There are a number of possible processes which may contribute to the observed differences, including chemically activated reactions of the nascent, internally excited RO radical,[37] changes in the barriers to reactions R2 and R3 due to solvation, and the possibility of additional chemistry in the condensed phase (e.g., an 1,2 H atom shift, which has been previously observed for some RO radicals in protic solvents[38−44]). Future work, including theoretical calculations, are necessary to better understand the origin of the observed change, and evaluate the extent to which this observation is generalizable to other RO systems.

4. CONCLUSIONS AND ATMOSPHERIC RELEVANCE

In this study, we have demonstrated the parallel analysis of gas- and condensed-phase products of RO and RO_2 radicals using a consistent methodology, allowing for direct comparisons of branching ratios across phases. The most striking difference is the enhancement in nitrate formation in the condensed phase. This enhancement has been previously reported in smaller peroxy radicals (C_1−C_4) in seawater.[24] Here, we present, to our knowledge, the first observation of this effect for a large and/or functionalized RO_2. Interestingly, the enhancement in X_{5a} observed in this work in the aqueous phase is considerably smaller than in other smaller RO_2 systems (Table 2), suggesting that size and/or functionality influences the RO_2 fate. This discrepancy also points to the need for further investigation of other large RO/RO_2 radicals, both through experiments and computational investigations.

The enhancement of nitrate yield from larger RO_2 may have an effect on the composition of atmospheric aerosols or droplets, and in particular on the composition of aqSOA. Moreover, since organic nitrates can serve as reservoir species for NO_x, this $RONO_2$ enhancement could have implications for the NO_x budget, affecting NO_x partitioning and hence ozone formation and radical cycling. Related to this, increased nitrate formation—as well as the enhanced carbonyl yield observed—result in an enhancement in chain termination steps in both condensed phases (this remains true even if the condensed-phase nitrate undergoes hydrolysis, forming an alcohol and HNO_3). This suggests that oxidation of organic species in the atmospheric condensed phase results in the formation of less-oxidized products than in the gas phase, and would require more oxidation steps (initiated by additional oxidants or UV light) to form highly oxidized products.

The degree to which these changes in condensed-phase product yields impact the chemistry of the atmosphere depends critically on the levels of NO in aqueous droplets and organic aerosol particles, since NO concentrations govern the rate of formation of RO radicals as well as RO_2 fate. Given the low Henry's Law solubility of NO,[45] partitioning of NO from the gas phase likely contributes negligibly to concentrations in the atmospheric condensed phase. However, NO can also be formed *in situ* from condensed-phase photolysis of inorganic nitrate and nitrite;[28,46] further study of these reactions, as well as the time scale of equilibration of solution-phase concentrations of NO, is important to quantitatively estimate condensed-phase NO concentrations in the atmosphere, and to understand the potential importance of condensed-phase RO_2 + NO reactions.

In addition, the underlying physical-chemical explanations for the observed dependence of branching ratios on phase remain uncertain. Computational study of the chemistry of RO and RO_2 radicals in both the gas phase and various condensed phases could provide important insight into these observations. Furthermore, chemical structure (carbon skeleton and functional groups) are known to have a governing influence on RO and RO_2 branching ratios,[22,23,47] and so other species may exhibit substantially different branching ratio enhancements in the condensed phase. The chemical environment is also likely to play a role, and future work on the impact of radical-solvent interactions (e.g., proton-exchange chemistry) and the presence of other radical and oxidant species would further clarify the importance of the observed effects in real atmospheric systems. Finally, chemistry within particles and droplets can be fundamentally different from that in bulk condensed-phase environments, due to differences in pH, mass transfer limitations, and surface effects; however it is unknown to what extent these effects will impact RO and RO_2 branching ratios. Detailed experimental and computational investigations of condensed-phase radicals are necessary to extend these results to the full range of organic compounds and condensed-phase environments found in the atmosphere.

https://doi.org/10.1021/acs.estlett.4c00473
Environ. Sci. Technol. Lett. 2024, 11, 975−980

■ ASSOCIATED CONTENT

Supporting Information

The Supporting Information is available free of charge at https://pubs.acs.org/doi/10.1021/acs.estlett.4c00473.

Additional details on experimental methods, including a diagram of the experimental setup; additional results, including an analysis of the pH dependence of *n*-pentyl nitrite hydrolysis, an analysis of tubing effects on the observed kinetics, and results of low-NO gas-phase experiments; a detailed derivation of the kinetic model used for extracting rate constants and branching ratios; a comparison between modeled and measured time profiles (PDF)

■ AUTHOR INFORMATION

Corresponding Authors

Victoria P. Barber − *Department of Civil and Environmental Engineering, Massachusetts Institute of Technology, Cambridge, Massachusetts 02139, United States;* Present Address: V.P.B.: Department of Chemistry and Biochemistry, University of California, Los Angeles, Los Angeles, CA, 90095, United States; orcid.org/0000-0003-4543-4657; Email: vbarber@chem.ucla.edu

Jesse H. Kroll − *Department of Civil and Environmental Engineering, Massachusetts Institute of Technology, Cambridge, Massachusetts 02139, United States; Department of Chemical Engineering, Massachusetts Institute of Technology, Cambridge, Massachusetts 02139, United States;* orcid.org/0000-0002-6275-521X; Email: jhkroll@mit.edu

Authors

Lexy N. LeMar − *Department of Chemical Engineering, Massachusetts Institute of Technology, Cambridge, Massachusetts 02139, United States*

Yaowei Li − *John A. Paulson School of Engineering and Applied Sciences, Harvard University, Cambridge, Massachusetts 02138, United States;* orcid.org/0000-0003-0725-6108

Jonathan W. Zheng − *Department of Chemical Engineering, Massachusetts Institute of Technology, Cambridge, Massachusetts 02139, United States*

Frank N. Keutsch − *John A. Paulson School of Engineering and Applied Sciences, Harvard University, Cambridge, Massachusetts 02138, United States;* orcid.org/0000-0002-1442-6200

Complete contact information is available at: https://pubs.acs.org/10.1021/acs.estlett.4c00473

Notes

The authors declare no competing financial interest.

■ ACKNOWLEDGMENTS

This work is supported by NSF grant CHE-210881. The authors gratefully acknowledge William H. Green (MIT), and Hartmut Herrmann and Erik H. Hoffmann (Leibniz-Institute for Tropospheric Research) for helpful discussions.

■ REFERENCES

(1) Hoffmann, E. H.; Tilgner, A.; Schrödner, R.; Bräuer, P.; Wolke, R.; Herrmann, H. An Advanced Modeling Study on the Impacts and Atmospheric Implications of Multiphase Dimethyl Sulfide Chemistry. *Proc. Natl. Acad. Sci. U. S. A.* **2016**, *113* (42), 11776−11781.

(2) George, I. J.; Abbatt, J. P. D. Heterogeneous Oxidation of Atmospheric Aerosol Particles by Gas-Phase Radicals. *Nat. Chem.* **2010**, *2* (9), 713−722.

(3) Lambe, A. T.; Cappa, C. D.; Massoli, P.; Onasch, T. B.; Forestieri, S. D.; Martin, A. T.; Cummings, M. J.; Croasdale, D. R.; Brune, W. H.; Worsnop, D. R.; Davidovits, P. Relationship between Oxidation Level and Optical Properties of Secondary Organic Aerosol. *Environ. Sci. Technol.* **2013**, *47* (12), 6349−6357.

(4) Galeazzo, T.; Valorso, R.; Li, Y.; Camredon, M.; Aumont, B.; Shiraiwa, M. Estimation of Secondary Organic Aerosol Viscosity from Explicit Modeling of Gas-Phase Oxidation of Isoprene and α-Pinene. *Atmospheric Chem. Phys.* **2021**, *21* (13), 10199−10213.

(5) Kroll, J. H.; Seinfeld, J. H. Chemistry of Secondary Organic Aerosol: Formation and Evolution of Low-Volatility Organics in the Atmosphere. *Atmos. Environ.* **2008**, *42* (16), 3593−3624.

(6) Calvert, J. G.; Derwent, R. G.; Orlando, J. J.; Wallington, T. J.; Tyndall, G. S. *Mechanisms of Atmospheric Oxidation of the Alkanes*; Oxford University Press: Oxford, NY, 2008.

(7) Atkinson, R.; Arey, J. Atmospheric Degradation of Volatile Organic Compounds. *Chem. Rev.* **2003**, *103* (12), 4605−4638.

(8) Calvert, J. G.; Mellouki, A.; Orlando, J. J. *Mechanisms of Atmospheric Oxidation of the Oxygenates*; Oxford University Press: Oxford, NY, 2011. DOI: 10.1093/oso/9780195365818.005.0001.

(9) Leviss, D. H.; Van Ry, D. A.; Hinrichs, R. Z. Multiphase Ozonolysis of Aqueous α-Terpineol. *Environ. Sci. Technol.* **2016**, *50* (21), 11698−11705.

(10) Akimoto, H.; Hirokawa, J. *Atmospheric Multiphase Chemistry: Fundamentals of Secondary Aerosol Formation*; John Wiley & Sons, 2020. DOI: 10.1002/9781119422419.

(11) Thornberry, T.; Abbatt, J. P. D. Heterogeneous Reaction of Ozone with Liquid Unsaturated Fatty Acids: Detailed Kinetics and Gas-Phase Product Studies. *Phys. Chem. Chem. Phys.* **2004**, *6* (1), 84−93.

(12) Adams, G. E.; Willson, R. L. Pulse Radiolysis Studies on the Oxidation of Organic Radicals in Aqueous Solution. *Trans. Faraday Soc.* **1969**, *65*, 2981.

(13) Schuchmann, M. N.; Von Sonntag, C. The Rapid Hydration of the Acetyl Radical. A Pulse Radiolysis Study of Acetaldehyde in Aqueous Solution. *J. Am. Chem. Soc.* **1988**, *110* (17), 5698−5701.

(14) Mezyk, S. P.; Elliot, A. J. Pulse Radiolysis of Iodate in Aqueous Solution. *J. Chem. Soc. Faraday Trans.* **1994**, *90* (6), 831−836.

(15) Lee, A. K. Y.; Zhao, R.; Gao, S. S.; Abbatt, J. P. D. Aqueous-Phase OH Oxidation of Glyoxal: Application of a Novel Analytical Approach Employing Aerosol Mass Spectrometry and Complementary Off-Line Techniques. *J. Phys. Chem. A* **2011**, *115* (38), 10517−10526.

(16) Carrasquillo, A. J.; Hunter, J. F.; Daumit, K. E.; Kroll, J. H. Secondary Organic Aerosol Formation via the Isolation of Individual Reactive Intermediates: Role of Alkoxy Radical Structure. *J. Phys. Chem. A* **2014**, *118* (38), 8807−8816.

(17) Kessler, S. H.; Nah, T.; Carrasquillo, A. J.; Jayne, J. T.; Worsnop, D. R.; Wilson, K. R.; Kroll, J. H. Formation of Secondary Organic Aerosol from the Direct Photolytic Generation of Organic Radicals. *J. Phys. Chem. Lett.* **2011**, *2* (11), 1295−1300.

(18) Iglesias, E.; Casado, J. Mechanisms of Hydrolysis and Nitrosation Reactions of Alkyl Nitrites in Various Media. *Int. Rev. Phys. Chem.* **2002**, *21* (1), 37−74.

(19) Hunter, J. F.; Carrasquillo, A. J.; Daumit, K. E.; Kroll, J. H. Secondary Organic Aerosol Formation from Acyclic, Monocyclic, and Polycyclic Alkanes. *Environ. Sci. Technol.* **2014**, *48* (17), 10227−10234.

(20) Zaytsev, A.; Breitenlechner, M.; Koss, A. R.; Lim, C. Y.; Rowe, J. C.; Kroll, J. H.; Keutsch, F. N. Using Collision-Induced Dissociation to Constrain Sensitivity of Ammonia Chemical Ionization Mass Spectrometry (NH_4^+ CIMS) to Oxygenated Volatile Organic Compounds. *Atmospheric Meas. Technol.* **2019**, *12* (3), 1861−1870.

(21) Orlando, J. J.; Tyndall, G. S.; Wallington, T. J. The Atmospheric Chemistry of Alkoxy Radicals. *Chem. Rev.* **2003**, *103* (12), 4657−4690.
(22) Atkinson, R. Rate Constants for the Atmospheric Reactions of Alkoxy Radicals: An Updated Estimation Method. *Atmos. Environ.* **2007**, *41* (38), 8468−8485.
(23) Jenkin, M. E.; Valorso, R.; Aumont, B.; Rickard, A. R. Estimation of Rate Coefficients and Branching Ratios for Reactions of Organic Peroxy Radicals for Use in Automated Mechanism Construction. *Atmospheric Chem. Phys.* **2019**, *19* (11), 7691−7717.
(24) Dahl, E. E.; Saltzman, E. S.; De Bruyn, W. J. The Aqueous Phase Yield of Alkyl Nitrates from ROO + NO: Implications for Photochemical Production in Seawater. *Geophys. Res. Lett.* **2003**, *30* (6), 1271.
(25) Butkovskaya, N.; Kukui, A.; Le Bras, G. Pressure and Temperature Dependence of Methyl Nitrate Formation in the CH_3O_2 + NO Reaction. *J. Phys. Chem. A* **2012**, *116* (24), 5972−5980.
(26) Richards-Henderson, N. K.; Goldstein, A. H.; Wilson, K. R. Large Enhancement in the Heterogeneous Oxidation Rate of Organic Aerosols by Hydroxyl Radicals in the Presence of Nitric Oxide. *J. Phys. Chem. Lett.* **2015**, *6* (22), 4451−4455.
(27) Renbaum, L. H.; Smith, G. D. Organic Nitrate Formation in the Radical-Initiated Oxidation of Model Aerosol Particles in the Presence of NO_x. *Phys. Chem. Chem. Phys.* **2009**, *11* (36), 8040−8047.
(28) Goldstein, S.; Lind, J.; Merenyi, G. Reaction of Organic Peroxyl Radicals with $^{\bullet}NO_2$ and $^{\bullet}NO$ in Aqueous Solution: Intermediacy of Organic Peroxynitrate and Peroxynitrite Species. *J. Phys. Chem. A* **2004**, *108* (10), 1719−1725.
(29) Butkovskaya, N.; Kukui, A.; Le Bras, G. Pressure and Temperature Dependence of Ethyl Nitrate Formation in the $C_2H_5O_2$ + NO Reaction. *J. Phys. Chem. A* **2010**, *114* (2), 956−964.
(30) Butkovskaya, N. I.; Kukui, A.; Le Bras, G. Pressure Dependence of Iso-Propyl Nitrate Formation in the i-$C_3H_7O_2$ + NO Reaction. *Z. Für Phys. Chem.* **2010**, *224* (7−8), 1025−1038.
(31) Atkinson, R.; Aschmann, S. M.; Carter, W. P. L.; Winer, A. M.; Pitts, J. N. Alkyl Nitrate Formation from the Nitrogen Oxide (NOx)-Air Photooxidations of C_2-C_8 *n*-Alkanes. *J. Phys. Chem.* **1982**, *86* (23), 4563−4569.
(32) Piletic, I. R.; Edney, E. O.; Bartolotti, L. J. Barrierless Reactions with Loose Transition States Govern the Yields and Lifetimes of Organic Nitrates Derived from Isoprene. *J. Phys. Chem. A* **2017**, *121* (43), 8306−8321.
(33) Aschmann, S. M.; Arey, J.; Atkinson, R. Atmospheric Chemistry of Selected Hydroxycarbonyls. *J. Phys. Chem. A* **2000**, *104* (17), 3998−4003.
(34) Barry, J. T.; Berg, D. J.; Tyler, D. R. Radical Cage Effects: The Prediction of Radical Cage Pair Recombination Efficiencies Using Microviscosity Across a Range of Solvent Types. *J. Am. Chem. Soc.* **2017**, *139* (41), 14399−14405.
(35) Pryor, W. A.; Squadrito, G. L. The Chemistry of Peroxynitrite: A Product from the Reaction of Nitric Oxide with Superoxide. *Am. J. Physiol.-Lung Cell. Mol. Physiol.* **1995**, *268* (5), L699−L722.
(36) Miyamoto, H.; Yampolski, Y.; Young, C. L. IUPAC-NIST Solubility Data Series. 103. Oxygen and Ozone in Water, Aqueous Solutions, and Organic Liquids (Supplement to Solubility Data Series Volume 7). *J. Phys. Chem. Ref. Data* **2014**, *43* (3), 033102.
(37) Sprague, M. K.; Garland, E. R.; Mollner, A. K.; Bloss, C.; Bean, B. D.; Weichman, M. L.; Mertens, L. A.; Okumura, M.; Sander, S. P. Kinetics of *n*-Butoxy and 2-Pentoxy Isomerization and Detection of Primary Products by Infrared Cavity Ringdown Spectroscopy. *J. Phys. Chem. A* **2012**, *116* (24), 6327−6340.
(38) Kamath, D.; Mezyk, S. P.; Minakata, D. Elucidating the Elementary Reaction Pathways and Kinetics of Hydroxyl Radical-Induced Acetone Degradation in Aqueous Phase Advanced Oxidation Processes. *Environ. Sci. Technol.* **2018**, *52* (14), 7763−7774.
(39) Elford, P. E.; Roberts, B. P. EPR Studies of the Formation and Transformation of Isomeric Radicals $[C_3H_5O]^{\bullet}$. Rearrangement of the Allyloxyl Radical in Non-Aqueous Solution Involving a Formal 1,2-Hydrogen-Atom Shift Promoted by Alcohols. *J. Chem. Soc., Perkin Trans.* **1996**, *2* (11), 2247−2256.
(40) Konya, K. G.; Paul, T.; Lin, S.; Lusztyk, J.; Ingold, K. U. Laser Flash Photolysis Studies on the First Superoxide Thermal Source. First Direct Measurements of the Rates of Solvent-Assisted 1,2-Hydrogen Atom Shifts and a Proposed New Mechanism for This Unusual Rearrangement. *J. Am. Chem. Soc.* **2000**, *122* (31), 7518−7527.
(41) Schuchmann, H.-P.; Sonntag, C. v. Methylperoxyl Radicals: A Study of the γ-Radiolysis of Methane in Oxygenated Aqueous Solutions. *Z. Für Naturforschung B* **1984**, *39* (2), 217−221.
(42) Schuchmann, H.-P.; von Sonntag, C. Photolysis at 185 nm of Dimethyl Ether in Aqueous Solution: Involvement of the Hydroxymethyl Radical. *J. Photochem.* **1981**, *16* (3), 289−295.
(43) von Sonntag, C.; Schuchmann, H.-P. The Elucidation of Peroxyl Radical Reactions in Aqueous Solution with the Help of Radiation-Chemical Methods. *Angew. Chem., Int. Ed. Engl.* **1991**, *30* (10), 1229−1253.
(44) Fernández-Ramos, A.; Zgierski, M. Z. Theoretical Study of the Rate Constants and Kinetic Isotope Effects of the 1,2-Hydrogen-Atom Shift of Methoxyl and Benzyloxyl Radicals Assisted by Water. *J. Phys. Chem. A* **2002**, *106* (44), 10578−10583.
(45) Sander, R. Compilation of Henry's Law Constants (Version 4.0) for Water as Solvent. *Atmospheric Chem. Phys.* **2015**, *15* (8), 4399−4981.
(46) Mack, J.; Bolton, J. R. Photochemistry of Nitrite and Nitrate in Aqueous Solution: A Review. *J. Photochem. Photobiol. Chem.* **1999**, *128* (1), 1−13.
(47) Méreau, R.; Rayez, M.-T.; Caralp, F.; Rayez, J.-C. Isomerisation Reactions of Alkoxy Radicals: Theoretical Study and Structure−Activity Relationships. *Phys. Chem. Chem. Phys.* **2003**, *5* (21), 4828−4833.

https://doi.org/10.1021/acs.estlett.4c00473
Environ. Sci. Technol. Lett. 2024, 11, 975−980